nature medicine

Chronic variable stress activates hematopoietic stem cells

Timo Heidt[1,7], Hendrik B Sager[1,7], Gabriel Courties[1], Partha Dutta[1], Yoshiko Iwamoto[1], Alex Zaltsman[1], Constantin von zur Muhlen[2], Christoph Bode[2], Gregory L Fricchione[3,4], John Denninger[3,4], Charles P Lin[1], Claudio Vinegoni[1], Peter Libby[5], Filip K Swirski[1], Ralph Weissleder[1,6] & Matthias Nahrendorf[1]

Exposure to psychosocial stress is a risk factor for many diseases, including atherosclerosis[1,2]. Although incompletely understood, interaction between the psyche and the immune system provides one potential mechanism linking stress and disease inception and progression. Known cross-talk between the brain and immune system includes the hypothalamic-pituitary-adrenal axis, which centrally drives glucocorticoid production in the adrenal cortex, and the sympathetic-adrenal-medullary axis, which controls stress-induced catecholamine release in support of the fight-or-flight reflex[3,4]. It remains unknown, however, whether chronic stress changes hematopoietic stem cell activity. Here we show that stress increases proliferation of these most primitive hematopoietic progenitors, giving rise to higher levels of disease-promoting inflammatory leukocytes. We found that chronic stress induced monocytosis and neutrophilia in humans. While investigating the source of leukocytosis in mice, we discovered that stress activates upstream hematopoietic stem cells. Under conditions of chronic variable stress in mice, sympathetic nerve fibers released surplus noradrenaline, which signaled bone marrow niche cells to decrease CXCL12 levels through the β_3-adrenergic receptor. Consequently, hematopoietic stem cell proliferation was elevated, leading to an increased output of neutrophils and inflammatory monocytes. When atherosclerosis-prone *Apoe*$^{-/-}$ mice were subjected to chronic stress, accelerated hematopoiesis promoted plaque features associated with vulnerable lesions that cause myocardial infarction and stroke in humans.

To explore the impact of stress on the human immune system, we analyzed blood samples from 29 medical residents working on a tertiary hospital intensive care unit (ICU), a challenging, fast-paced work environment that frequently includes the responsibility of life-or-death decisions. Compared to when off duty, residents working on the ICU reported an increased stress perception, which we assessed with Cohen's Perceived Stress Scale[5] (**Fig. 1a**). Visual analog scales[6] documented a higher stress intensity and frequency while working on the ICU (**Supplementary Fig. 1a**). When comparing samples taken during work to samples taken off duty, we observed an increase in blood leukocytes (**Fig. 1b**), with higher numbers of neutrophils, monocytes and lymphocytes, after 1 week of intensive care rotation (**Supplementary Fig. 1b**). The relative frequencies of monocyte subsets did not change (**Supplementary Fig. 1c**).

To test the hypothesis that stress-induced leukocytosis results from increased leukocyte production, we exposed wild-type mice to chronic variable stressors validated by behavioral neuroscience studies (**Supplementary Table 1**)[7–9]. Compared to nonstressed controls, stressed mice had increased numbers of leukocytes, neutrophils and monocytes in blood (**Fig. 1c**), which is consistent with our observations in humans. These cells were also more numerous in the bone marrow (**Fig. 1d**). We next investigated the influence of chronic stress on blood cell production in the bone marrow and detected increased cycling of Lin$^-$Sca-1$^+$c-Kit$^+$CD150$^+$CD48$^-$ hematopoietic stem cells[10] (HSCs, **Fig. 1e**), which also incorporated increased amounts of BrdU (**Supplementary Fig. 2a**). To assess HSC quiescence, we performed a pulse-chase BrdU label retention experiment. BrdU exposure in drinking water for 2 weeks led to >90% labeling of HSCs, as previously reported[11]. After completion of the labeling phase, we stressed mice for 3 weeks, which accelerated HSC BrdU washout when compared to nonstressed controls (**Supplementary Fig. 2b**). Bone marrow harvested from stressed mice had augmented colony-forming capacity, indicative of increased progenitor cell proliferation (**Fig. 1f**). Enhanced proliferation resulted in higher bone marrow numbers of HSCs, Lin$^-$Sca-1$^+$c-Kit$^+$ progenitors (LSKs, **Fig. 1g**), granulocyte macrophage progenitors, macrophage dendritic cell progenitors (**Supplementary Fig. 3a**) and common lymphoid progenitors (**Supplementary Fig. 3b**).

Although CD150$^+$CD48$^-$ SLAM staining phenotypically quantitates HSCs, only a fraction of the cells in this gate are functional long-term HSCs (LT-HSCs)[10]. A competitive repopulation assay[12] comparing limiting bone marrow dilutions obtained from stressed and nonstressed donors indicated that the frequency of LT-HSCs did not significantly change in stressed mice (**Fig. 1h** and **Supplementary Table 2**). When viewed together with the increased bone marrow cellularity in stressed mice (1.64×10^7 versus 2.46×10^7 per femur, $P < 0.0001$, $n = 14$ control mice, $n = 18$ stressed mice), our results

[1]Center for Systems Biology, Massachusetts General Hospital and Harvard Medical School, Boston, Massachusetts, USA. [2]Department of Cardiology and Angiology I, University Heart Center, Freiburg, Germany. [3]Division of Psychiatry and Medicine, Massachusetts General Hospital, Boston, Massachusetts, USA. [4]Benson-Henry Institute for Mind Body Medicine, Massachusetts General Hospital, Boston, Massachusetts, USA. [5]Cardiovascular Division, Department of Medicine, Brigham and Women's Hospital, Boston, Massachusetts, USA. [6]Department of Systems Biology, Harvard Medical School, Boston, Massachusetts, USA. [7]These authors contributed equally to this work. Correspondence should be addressed to M.N. (mnahrendorf@mgh.harvard.edu).

Received 30 March; accepted 12 May; published online 22 June 2014; doi:10.1038/nm.3589

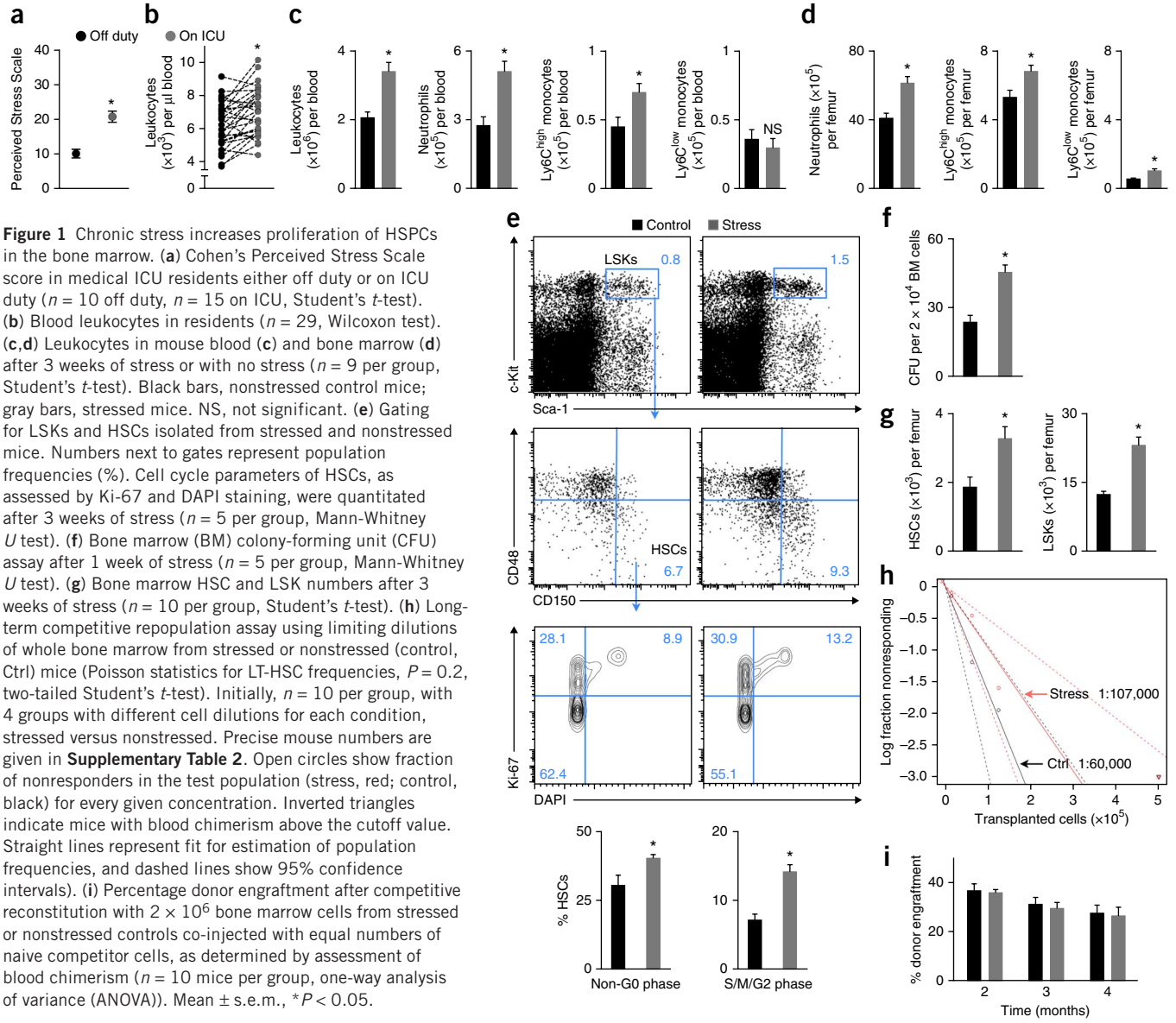

Figure 1 Chronic stress increases proliferation of HSPCs in the bone marrow. (**a**) Cohen's Perceived Stress Scale score in medical ICU residents either off duty or on ICU duty ($n = 10$ off duty, $n = 15$ on ICU, Student's t-test). (**b**) Blood leukocytes in residents ($n = 29$, Wilcoxon test). (**c**,**d**) Leukocytes in mouse blood (**c**) and bone marrow (**d**) after 3 weeks of stress or with no stress ($n = 9$ per group, Student's t-test). Black bars, nonstressed control mice; gray bars, stressed mice. NS, not significant. (**e**) Gating for LSKs and HSCs isolated from stressed and nonstressed mice. Numbers next to gates represent population frequencies (%). Cell cycle parameters of HSCs, as assessed by Ki-67 and DAPI staining, were quantitated after 3 weeks of stress ($n = 5$ per group, Mann-Whitney U test). (**f**) Bone marrow (BM) colony-forming unit (CFU) assay after 1 week of stress ($n = 5$ per group, Mann-Whitney U test). (**g**) Bone marrow HSC and LSK numbers after 3 weeks of stress ($n = 10$ per group, Student's t-test). (**h**) Long-term competitive repopulation assay using limiting dilutions of whole bone marrow from stressed or nonstressed (control, Ctrl) mice (Poisson statistics for LT-HSC frequencies, $P = 0.2$, two-tailed Student's t-test). Initially, $n = 10$ per group, with 4 groups with different cell dilutions for each condition, stressed versus nonstressed. Precise mouse numbers are given in **Supplementary Table 2**. Open circles show fraction of nonresponders in the test population (stress, red; control, black) for every given concentration. Inverted triangles indicate mice with blood chimerism above the cutoff value. Straight lines represent fit for estimation of population frequencies, and dashed lines show 95% confidence intervals). (**i**) Percentage donor engraftment after competitive reconstitution with 2×10^6 bone marrow cells from stressed or nonstressed controls co-injected with equal numbers of naive competitor cells, as determined by assessment of blood chimerism ($n = 10$ mice per group, one-way analysis of variance (ANOVA)). Mean ± s.e.m., $^*P < 0.05$.

suggest that stress neither increases nor exhausts LT-HSCs. An unchanged number of LT-HSCs in stressed mice is further supported by comparable blood chimerism 16 weeks after transfer of 2×10^6 bone marrow cells from either stressed or nonstressed donors with equal numbers of naive competitor cells into lethally irradiated recipients (**Fig. 1i**). In contrast, infection and interferons increase HSC proliferation while exhausting LT-HSCs[13] or impairing their engraftment[14], possibly because these stimuli are more severe than chronic stress. Of note, interferon protein levels were unchanged in the bone marrow of stressed mice (**Supplementary Fig. 4a**).

To test whether leukocyte production or redistribution was the source of stress-induced leukocytosis, we performed a 5-fluorouracil (5-FU) challenge, a treatment that kills actively cycling progenitor cells. 5-FU completely abolished stress-induced leukocytosis, suggesting that the observed leukocytosis is caused by progenitor proliferation. Notably, stressed mice had an enhanced leukocyte rebound on day 14 after 5-FU injection, which was probably caused by increased cycling of hematopoietic progenitors (**Supplementary Fig. 4b**). Serial intravital microscopy[15] in the calvarium of mice that had undergone adoptive transfer of 25,000 1,1′-dioctadecyl-3,3,3′,3′-tetramethylindodicarbocyanine perchlorate (DiD)-labeled LSKs detected accelerated dilution of the membrane dye in mice exposed to 7 d of stress (**Fig. 2a**), indicating accentuated cell proliferation. Flow cytometry confirmed the accelerated membrane dye dilution after stress exposure (**Fig. 2b**). Taken together, these data indicate that chronic stress activates HSCs, which increase proliferation and differentiate into downstream progenitors.

Noradrenaline is a prototypical stress hormone that also regulates circadian progenitor cell migration[16] and proliferation[17,18]. We wondered whether heightened hematopoietic system activity during stress could be related to this catecholamine. Indeed, noradrenaline levels increased in the bone marrow of stressed mice compared to nonstressed controls (**Fig. 3a**). Immunoreactive staining for tyrosine hydroxylase, a rate-limiting enzyme for noradrenaline synthesis[19], rose in sympathetic nerve fibers surrounding blood vessels in the bone marrow (**Fig. 3b**). This rise was associated with a sharp decrease in CXCL12 mRNA and protein within whole bone marrow (**Fig. 3c**,**d**), in line with the role of noradrenaline in regulating CXCL12 synthesis[16].

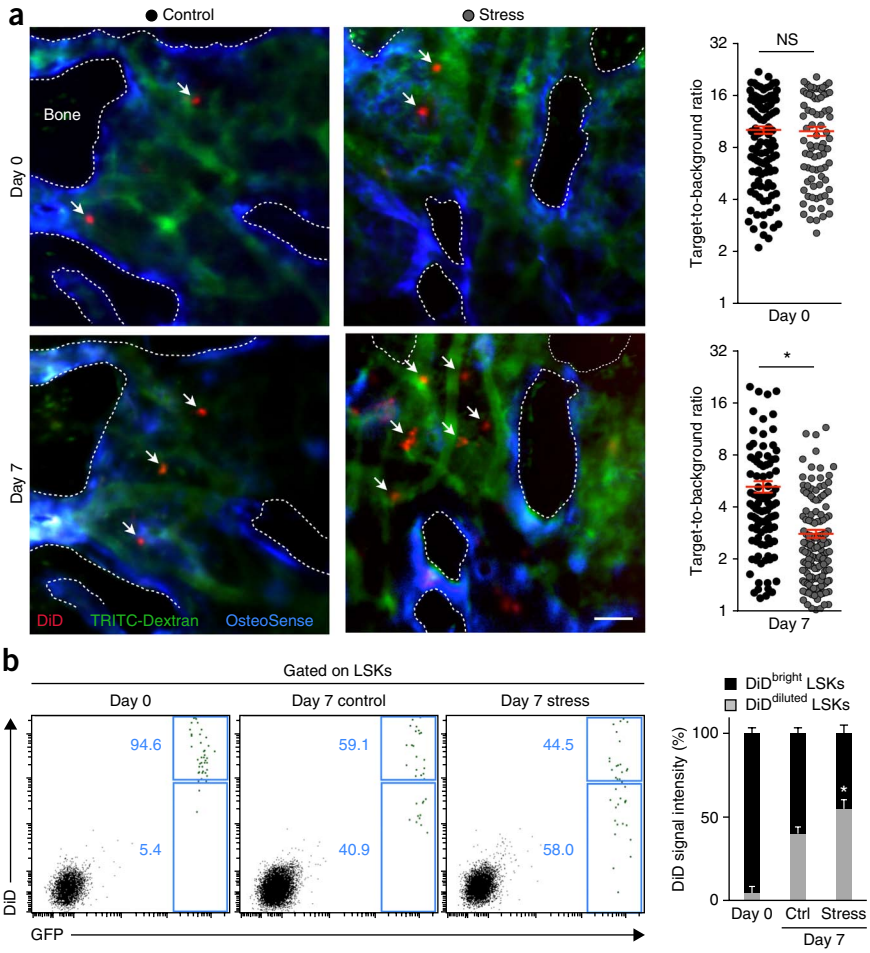

Figure 2 Stress leads to increased bone marrow hematopoietic progenitor cell proliferation. (**a**) Intravital microscopy of the mouse calvarium after adoptive transfer of DiD-labeled LSKs (white arrows) before (day 0) and 7 d after stress ($n = 5$ mice per group, Mann-Whitney U test). Dotted lines outline bone. Scale bar, 50 µm. Each dot in the graphs represents the target-to-background ratio of DiD$^+$ cells either before (top) or after stress (bottom). (**b**) DiD fluorescence after adoptive transfer of DiD$^+$GFP$^+$ LSKs in nonstressed control (Ctrl) or stressed mice ($n = 5$ per group). The bar graph quantitates DiD fluorescence in GFP$^+$ LSKs (Mann-Whitney U test). Mean ± s.e.m., $^*P < 0.05$. NS, not significant.

Conditional deletion of tyrosine hydroxylase–containing cells in cross-bred iDTR TH-Cre mice[18] preserved CXCL12 levels after stress exposure and blunted the bone marrow stress response when compared to stressed wild-type mice (**Supplementary Fig. 5**).

In the hematopoietic niche, CXCL12 derives from mesenchymal stem cells, osteoblasts and endothelial cells[20–22]. Its primary functions include inhibiting hematopoietic stem and progenitor cell (HSPC) proliferation and migration; it also retains neutrophils in the bone marrow[23]. CXCL12-deficient mice[24] and mice that lack the chemokine's cognate receptor (CXCR4)[25] show increased HSC cycling and progenitor pool expansion and increased neutrophil release into circulation compared to wild-type mice. Linking the autonomic nervous system and leukocyte trafficking, the β_3-adrenergic receptor expressed on niche cells regulates CXCL12 release[16]. Among relevant niche cells, we found that mesenchymal stem cells express the highest level of the β_3 receptor (**Supplementary Fig. 6**). We therefore investigated whether chronic stress acts on hematopoiesis via the β_3-adrenergic receptor. Indeed, mice with a genetic lack of the receptor were protected from stress, as CXCL12 expression and HSC cycling were similar in stressed and nonstressed *Adrb3*$^{-/-}$ mice (**Supplementary Fig. 7**). Moreover, treatment of stressed wild-type mice with the β_3-selective receptor blocker SR 59230A restored CXCL12 mRNA and protein levels (**Fig. 3c**,**d**), decreased BrdU incorporation into HSCs and reduced HSPC numbers in the bone marrow (**Fig. 3e**,**f**). As a consequence, downstream granulocyte macrophage progenitor and macrophage dendritic cell progenitor numbers fell (**Supplementary Fig. 8a**), resulting in lower levels of neutrophils and Ly6C^{high} monocytes in circulation (**Fig. 3g**). In contrast, treatment with a β_2 receptor blocker failed to protect the bone marrow against stress (**Supplementary Fig. 8b**,**c**).

Atherosclerosis is a chronic inflammatory disease driven by hyperlipidemia[26–28]. Atherosclerotic plaques consist of cholesterol deposits and a leukocyte infiltrate that is dominated by innate immune cells[29]. Inflammatory monocyte and macrophage infiltration may lead to plaque rupture, myocardial infarction and stroke[30,31], and higher blood levels of monocytes and neutrophils correlate with increased mortality[29,32]. Proteases released from inflammatory leukocytes weaken the fibrous cap and favor plaque disruption that permits contact between the plaque's necrotic core and clotting factors in the bloodstream, inciting local thrombosis and thereby jeopardizing oxygen supply to the heart and brain[30,33]. A number of risk factors contribute to inflammatory complications of atherosclerosis. Chronic stress is well recognized among them[4,34–37]. Yet, the mechanisms that link chronic stress to higher cardiovascular event rates are incompletely understood.

We decided to test the hypothesis that chronic stress acts on the bone marrow via sympathetic nervous system activity to increase inflammatory leukocyte supply to atherosclerotic lesions. Exposure to 6 weeks of stress enhanced hematopoietic system activity in atherosclerosis-prone *Apoe*$^{-/-}$ mice, as indicated by increased BrdU incorporation into HSCs and higher numbers of granulocyte macrophage progenitors and macrophage dendritic cell progenitors in the femur (**Supplementary Fig. 9a**,**b**), whereas body weight and lipid levels were unaffected (**Supplementary Fig. 9c**,**d**). Plaque protease levels increased, as assessed by fluorescence molecular tomography–computed tomography (FMT-CT) imaging (**Fig. 4a**). Innate immune cells are largely responsible for protease production in atherosclerotic plaque[29,30]. Accordingly, in stressed *Apoe*$^{-/-}$ mice, we detected higher CD11b$^+$ myeloid cell and neutrophil content in plaque by histology (**Fig. 4b**) and increased numbers of neutrophils, monocytes and macrophages in whole aortas by flow cytometry (**Fig. 4c**). Neutrophils may aid monocyte entry into plaque[38] but can also have inflammatory functions themselves[39]. The aortic arches of *Apoe*$^{-/-}$ mice exhibited an inflammatory cytokine expression profile after stress (**Fig. 4d**), including increased expression of myeloperoxidase, a pro-oxidant enzyme abundant in neutrophils and inflammatory monocytes.

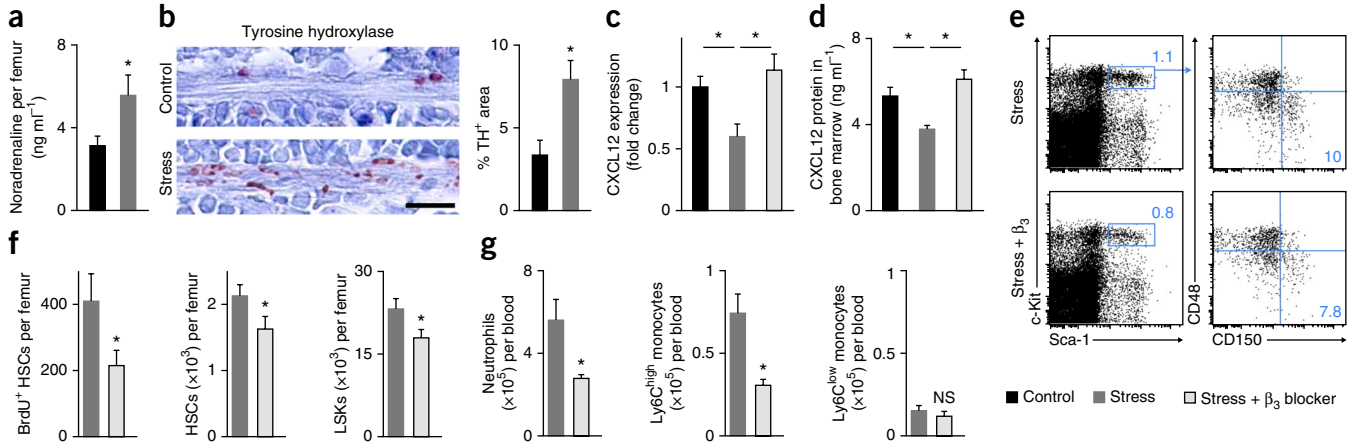

Figure 3 Stress-induced sympathetic nervous system signaling regulates the proliferation of bone marrow HSCs via CXCL12. (**a**) Noradrenaline levels, as assessed by ELISA, after 3 weeks of stress ($n = 8$ per group, Student's t-test). (**b**) Immunoreactive staining for tyrosine hydroxylase (TH) in bone marrow. Scale bar, 10 μm. The bar graph shows the percentage of TH-positive area per field of view ($n = 5$ mice per group, Mann-Whitney U test). (**c**) CXCL12 mRNA in bone marrow of nonstressed, stressed and stressed mice treated with a β_3-selective receptor blocker ($n = 10$ per group, one-way ANOVA). (**d**) CXCL12 protein in bone marrow ($n = 7$ per group, one-way ANOVA). (**e**) Gating of LSKs (left) and HSCs (right). (**f**,**g**) Quantitation of BrdU incorporation and absolute cell numbers (**f**) and effects of a β_3-adrenergic receptor blocker on the indicated populations of blood leukocytes (**g**) ($n = 5$ per group, Mann-Whitney U test). Mean ± s.e.m., $^*P < 0.05$. NS, not significant.

Whereas aortic root plaque size did not change in stressed versus nonstressed *Apoe*$^{-/-}$ mice (**Supplementary Fig. 10**), the inflammatory milieu in the stressed mice led to thinner fibrous caps and larger necrotic plaque cores (**Fig. 4e**), hallmarks of rupture-prone lesions in patients with acute myocardial infarction or stroke[29,33]. Heightened recruitment of leukocytes into plaques may also result from enhanced action of adhesion molecules; however, the mRNA and protein levels of the adhesion molecules, with the exception of E-selectin, were unchanged in stressed *Apoe*$^{-/-}$ mice (**Supplementary Fig. 11a**,**b**). When we adoptively transferred equal numbers of GFP$^+$ myeloid cells into stressed and nonstressed *Apoe*$^{-/-}$ mice, we detected similar recruitment of these cells to plaques (**Supplementary Fig. 11c**), indicating that stress acts through increased systemic leukocyte supply by the hematopoietic system rather than locally increased cell recruitment. Hypertension, a known risk factor for atherosclerosis, occurred only during stress exposure (**Supplementary Fig. 12a**) and therefore probably did not play a dominant role in the observed disease progression. Blood pressure, cholesterol and corticosterone levels were unchanged in stressed *Apoe*$^{-/-}$ mice that received a β_3-adrenergic receptor blocker (**Supplementary Fig. 12b**,**c**); however, this treatment reduced the number of neutrophils, inflammatory monocytes and macrophages in plaque, providing a direct link between

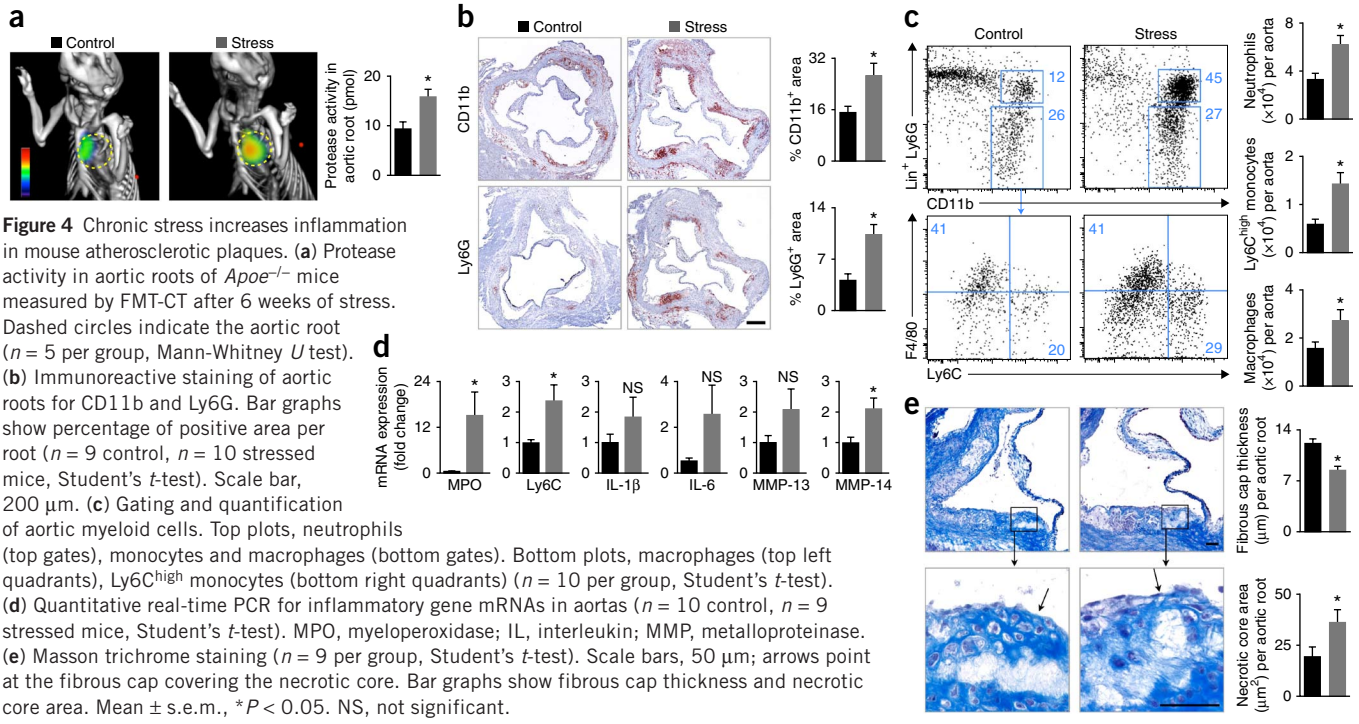

Figure 4 Chronic stress increases inflammation in mouse atherosclerotic plaques. (**a**) Protease activity in aortic roots of *Apoe*$^{-/-}$ mice measured by FMT-CT after 6 weeks of stress. Dashed circles indicate the aortic root ($n = 5$ per group, Mann-Whitney U test). (**b**) Immunoreactive staining of aortic roots for CD11b and Ly6G. Bar graphs show percentage of positive area per root ($n = 9$ control, $n = 10$ stressed mice, Student's t-test). Scale bar, 200 μm. (**c**) Gating and quantification of aortic myeloid cells. Top plots, neutrophils (top gates), monocytes and macrophages (bottom gates). Bottom plots, macrophages (top left quadrants), Ly6C^{high} monocytes (bottom right quadrants) ($n = 10$ per group, Student's t-test). (**d**) Quantitative real-time PCR for inflammatory gene mRNAs in aortas ($n = 10$ control, $n = 9$ stressed mice, Student's t-test). MPO, myeloperoxidase; IL, interleukin; MMP, metalloproteinase. (**e**) Masson trichrome staining ($n = 9$ per group, Student's t-test). Scale bars, 50 μm; arrows point at the fibrous cap covering the necrotic core. Bar graphs show fibrous cap thickness and necrotic core area. Mean ± s.e.m., $^*P < 0.05$. NS, not significant.

hematopoietic progenitor activity and atherosclerotic plaque inflammation (**Supplementary Fig. 13**).

In summary, we report how chronic stress interferes with hematopoiesis and describe interactions between the central nervous system, immunity and atherosclerosis. In mice exposed to stress, increased sympathetic nervous system activity decreased CXCL12 expression in the hematopoietic stem cell niche, accelerated HSC proliferation and enhanced neutrophil and monocyte production. These events caused extensive release of inflammatory leukocytes into the circulation and promoted plaque inflammation. Administration of a β_3-adrenergic receptor blocker limited disease progression, supporting the notion that sympathetic nervous system signaling via this receptor and targeting of the CXCL12-CXCR4 interaction in the bone marrow should be explored as potential therapeutic avenues.

The data obtained in mice parallel our observations in ICU residents; however, we interpret this association with care, as the nature and the timing of the stress differed. Further, we were unable to investigate HSC activity in stressed humans. Taken together, these data provide further evidence of the hematopoietic system's role in cardiovascular disease[29,40] and elucidate a direct biological link between chronic variable stress and chronic inflammation, a general concept with implications beyond atherosclerosis.

METHODS

Methods and any associated references are available in the online version of the paper.

Note: Any Supplementary Information and Source Data files are available in the online version of the paper.

ACKNOWLEDGMENTS

We thank the team at the Center for Systems Biology Mouse Imaging Program, especially J. Truelove and D. Jeon, for help with imaging, M. Stein, I. Neudorfer and F. Meixner for help with the clinical study and L. Prickett-Rice, K. Folz-Donahue, M. Weglarz, M. Waring and A. Chicoine for assistance with cell sorting. We thank P. Frenette (Albert Einstein College of Medicine) and B. Lowell (Beth Israel Deaconess Medical Center) for providing *Adrb3*$^{-/-}$ mice and G. Enikolopov (Cold Spring Harbor Laboratory) for providing nestin-GFP mice. We thank the ICU team at the University Hospital Freiburg, Germany. This work was funded in part by US National Institutes of Health grants R01-HL114477, R01-HL117829 and R01-HL096576 (to M.N.) and grant HHSN268201000044C (to R.W.). T.H. and H.B.S. are funded by the Deutsche Forschungsgemeinschaft (HE-6382/1-1 to T.H. and SA1668/2-1 to H.B.S.).

AUTHOR CONTRIBUTIONS

T.H. and H.B.S. performed experiments, collected, analyzed and discussed data and contributed to writing the manuscript. G.C., P.D., A.Z. and Y.I. performed experiments and collected, analyzed and discussed data. C.v.z.M., C.B., C.P.L., J.D., G.L.F., C.V., P.L., F.K.S. and R.W. conceived experiments and discussed results and strategy. M.N. managed and designed the study and wrote the manuscript, which was revised and approved by all authors.

COMPETING FINANCIAL INTERESTS

The authors declare no competing financial interests.

1. Black, P.H. The inflammatory response is an integral part of the stress response: implications for atherosclerosis, insulin resistance, type II diabetes and metabolic syndrome X. *Brain Behav. Immun.* **17**, 350–364 (2003).
2. Rosengren, A. *et al.* Association of psychosocial risk factors with risk of acute myocardial infarction in 11119 cases and 13648 controls from 52 countries (the INTERHEART study): case-control study. *Lancet* **364**, 953–962 (2004).
3. Glaser, R. & Kiecolt-Glaser, J.K. Stress-induced immune dysfunction: implications for health. *Nat. Rev. Immunol.* **5**, 243–251 (2005).
4. Powell, N.D. *et al.* Social stress up-regulates inflammatory gene expression in the leukocyte transcriptome via β-adrenergic induction of myelopoiesis. *Proc. Natl. Acad. Sci. USA* **110**, 16574–16579 (2013).
5. Cohen, S., Kamarck, T. & Mermelstein, R. A global measure of perceived stress. *J. Health Soc. Behav.* **24**, 385–396 (1983).
6. Lesage, F.X. & Berjot, S. Validity of occupational stress assessment using a visual analogue scale. *Occup. Med.* (*Lond.*) **61**, 434–436 (2011).
7. Schweizer, M.C., Henniger, M.S. & Sillaber, I. Chronic mild stress (CMS) in mice: of anhedonia, 'anomalous anxiolysis' and activity. *PLoS ONE* **4**, e4326 (2009).
8. Nollet, M., Guisquet, A.M. & Belzung, C. Models of depression: unpredictable chronic mild stress in mice. *Curr. Protoc. Pharmacol.* **61**, 5.65 (2013).
9. Yalcin, I., Aksu, F. & Belzung, C. Effects of desipramine and tramadol in a chronic mild stress model in mice are altered by yohimbine but not by pindolol. *Eur. J. Pharmacol.* **514**, 165–174 (2005).
10. Kiel, M.J. *et al.* SLAM family receptors distinguish hematopoietic stem and progenitor cells and reveal endothelial niches for stem cells. *Cell* **121**, 1109–1121 (2005).
11. Wilson, A. *et al.* Hematopoietic stem cells reversibly switch from dormancy to self-renewal during homeostasis and repair. *Cell* **135**, 1118–1129 (2008).
12. Szilvassy, S.J., Humphries, R.K., Lansdorp, P.M., Eaves, A.C. & Eaves, C.J. Quantitative assay for totipotent reconstituting hematopoietic stem cells by a competitive repopulation strategy. *Proc. Natl. Acad. Sci. USA* **87**, 8736–8740 (1990).
13. Essers, M.A. *et al.* IFNα activates dormant haematopoietic stem cells *in vivo*. *Nature* **458**, 904–908 (2009).
14. Baldridge, M.T., King, K.Y., Boles, N.C., Weksberg, D.C. & Goodell, M.A. Quiescent haematopoietic stem cells are activated by IFN-γ in response to chronic infection. *Nature* **465**, 793–797 (2010).
15. Lo Celso, C., Lin, C.P. & Scadden, D.T. *In vivo* imaging of transplanted hematopoietic stem and progenitor cells in mouse calvarium bone marrow. *Nat. Protoc.* **6**, 1–14 (2011).
16. Méndez-Ferrer, S., Lucas, D., Battista, M. & Frenette, P.S. Haematopoietic stem cell release is regulated by circadian oscillations. *Nature* **452**, 442–447 (2008).
17. Spiegel, A. *et al.* Catecholaminergic neurotransmitters regulate migration and repopulation of immature human CD34$^+$ cells through Wnt signaling. *Nat. Immunol.* **8**, 1123–1131 (2007).
18. Lucas, D. *et al.* Chemotherapy-induced bone marrow nerve injury impairs hematopoietic regeneration. *Nat. Med.* **19**, 695–703 (2013).
19. Zigmond, R.E. & Ben-Ari, Y. Electrical stimulation of preganglionic nerve increases tyrosine hydroxylase activity in sympathetic ganglia. *Proc. Natl. Acad. Sci. USA* **74**, 3078–3080 (1977).
20. Morrison, S.J. & Scadden, D.T. The bone marrow niche for haematopoietic stem cells. *Nature* **505**, 327–334 (2014).
21. Méndez-Ferrer, S. *et al.* Mesenchymal and haematopoietic stem cells form a unique bone marrow niche. *Nature* **466**, 829–834 (2010).
22. Ding, L. & Morrison, S.J. Haematopoietic stem cells and early lymphoid progenitors occupy distinct bone marrow niches. *Nature* **495**, 231–235 (2013).
23. Eash, K.J., Means, J.M., White, D.W. & Link, D.C. CXCR4 is a key regulator of neutrophil release from the bone marrow under basal and stress granulopoiesis conditions. *Blood* **113**, 4711–4719 (2009).
24. Tzeng, Y.S. *et al.* Loss of Cxcl12/Sdf-1 in adult mice decreases the quiescent state of hematopoietic stem/progenitor cells and alters the pattern of hematopoietic regeneration after myelosuppression. *Blood* **117**, 429–439 (2011).
25. Nie, Y., Han, Y.C. & Zou, Y.R. CXCR4 is required for the quiescence of primitive hematopoietic cells. *J. Exp. Med.* **205**, 777–783 (2008).
26. Libby, P., Ridker, P.M. & Hansson, G.K. Progress and challenges in translating the biology of atherosclerosis. *Nature* **473**, 317–325 (2011).
27. Randolph, G.J. The fate of monocytes in atherosclerosis. *J. Thromb. Haemost.* **7** (suppl. 1), 28–30 (2009).
28. Rader, D.J. & Daugherty, A. Translating molecular discoveries into new therapies for atherosclerosis. *Nature* **451**, 904–913 (2008).
29. Swirski, F.K. & Nahrendorf, M. Leukocyte behavior in atherosclerosis, myocardial infarction, and heart failure. *Science* **339**, 161–166 (2013).
30. Moore, K.J. & Tabas, I. Macrophages in the pathogenesis of atherosclerosis. *Cell* **145**, 341–355 (2011).
31. Libby, P. Mechanisms of acute coronary syndromes and their implications for therapy. *N. Engl. J. Med.* **368**, 2004–2013 (2013).
32. Adamsson Eryd, S., Smith, J.G., Melander, O., Hedblad, B. & Engstrom, G. Incidence of coronary events and case fatality rate in relation to blood lymphocyte and neutrophil counts. *Arterioscler. Thromb. Vasc. Biol.* **32**, 533–539 (2012).
33. Libby, P. Inflammation in atherosclerosis. *Nature* **420**, 868–874 (2002).
34. Kaplan, J.R. *et al.* Social stress and atherosclerosis in normocholesterolemic monkeys. *Science* **220**, 733–735 (1983).
35. Gu, H., Tang, C., Peng, K., Sun, H. & Yang, Y. Effects of chronic mild stress on the development of atherosclerosis and expression of toll-like receptor 4 signaling pathway in adolescent apolipoprotein E knockout mice. *J. Biomed. Biotechnol.* **2009**, 613879 (2009).
36. Bernberg, E., Ulleryd, M.A., Johansson, M.E. & Bergstrom, G.M. Social disruption stress increases IL-6 levels and accelerates atherosclerosis in *Apoe*$^{-/-}$ mice. *Atherosclerosis* **221**, 359–365 (2012).
37. Wilbert-Lampen, U. *et al.* Cardiovascular events during World Cup soccer. *N. Engl. J. Med.* **358**, 475–483 (2008).
38. Wantha, S. *et al.* Neutrophil-derived cathelicidin promotes adhesion of classical monocytes. *Circ. Res.* **112**, 792–801 (2013).
39. Weber, C. & Noels, H. Atherosclerosis: current pathogenesis and therapeutic options. *Nat. Med.* **17**, 1410–1422 (2011).
40. Tall, A.R., Yvan-Charvet, L., Westerterp, M. & Murphy, A.J. Cholesterol efflux: a novel regulator of myelopoiesis and atherogenesis. *Arterioscler. Thromb. Vasc. Biol.* **32**, 2547–2552 (2012).

ONLINE METHODS

Clinical study. The clinical study titled 'Effects of Socioenvironmental Stress on the Human Hematopoietic System' was an open, monocenter, single-arm study that enrolled medical residents working on the intensive care unit at University Hospital, Freiburg, Germany. This study was registered with the German Registry for Clinical Studies (DRKS00004821) and was approved by the Ethics Committee of Albert-Ludwigs-University Freiburg, Germany (No. 52/13). All residents working on the ICU were considered eligible to participate in the study. Exclusion criteria were smoking, any acute or chronic illness, regular intake of medication or failure to consent. Twenty-nine volunteers (23 male, 6 female, mean age 33.7 ± 0.8 years) were enrolled after signing the informed consent form. Residents gave two blood samples (baseline and stress). The off-duty sample (baseline) was collected after 10 ± 0.9 consecutive days off duty. The on-duty sample (stress) was collected after 7 ± 0.3 consecutive days of ICU duty. A subcohort of participants completed the Perceived Stress Scale 10-item inventory[5] before starting to work on the ICU (baseline), as well as after several weeks on duty (stress). Short-term perception for stress frequency and intensity was measured with visual analog scales (scale 0–10)[6], which each participant completed at the time of the blood sampling. The mean circadian time difference between the baseline and the stress sample was 20 ± 15.9 min. Blood samples were analyzed in a blinded fashion at the routine clinical laboratory of the University Hospital, Freiburg, Germany.

Mice. We used C57BL/6, CD45.1 (B6.SJL-*Ptprca Pepcb*/BoyJ), UBC-GFP (C57BL/6-Tg(UBC-GFP)30Scha/J), *Apoe*$^{-/-}$ (B6.129P2-Apoetm1Unc/J), TH-Cre (B6.Cg-Tg(Th-Cre)1Tmd/J) and iDTR (C57BL/6-Gt(ROSA)26Sor$^{tm1(HBEGF)Awai}$/J) mice, all female and 10–12 weeks of age (Jackson Laboratories, Bar Harbor, ME). *Adrb3*$^{-/-}$ mice[16] were donated by P. Frenette (Albert Einstein College of Medicine, New York, NY, USA) and B. Lowell (Beth Israel Deaconess Medical Center, Boston, MA, USA). Nestin-GFP mice[41] were a gift from G. Enikolopov (Cold Spring Harbor Laboratory, NY). All procedures were approved by the Subcommittee on Animal Research Care at Massachusetts General Hospital. For each experiment, age-matched female littermates were randomly allocated to study groups. Animal studies were performed without blinding of the investigator.

Stress procedures. Mice were exposed to socioenvironmental stressors[7–9] for one or three weeks in C57BL/6 mice or six weeks in *Apoe*$^{-/-}$ mice. Stress procedures were performed between 7 a.m. and 6 p.m. The following stressors were applied. For cage tilt, the cage was tilted at a 45° angle and kept in this position for six hours. For isolation, mice were individually housed in an area one-quarter of the original cage size (12 cm × 8 cm) for four hours, followed by crowding, during which 10 animals were housed in one cage for two hours. Mice were monitored during the crowding procedure, and 'fighters' were separated. For damp bedding, water was added to the cage to moisten the bedding without generating large pools. Mice were kept for six hours with damp bedding. For rapid light-dark changes, using an automatic timer, the light was switched with an interval of seven minutes for two hours. For overnight illumination, mice were housed in a separate room with illumination from 7 p.m. to 7 a.m. All stressors were randomly shuffled in consecutive weeks. Efficacy of the chronic stress procedures was confirmed by measurement of blood corticosterone levels (**Supplementary Fig. 12c**).

Lethal irradiation. Mice were irradiated using a split dose of 2 × 600 cGy with an interval of 3 h between doses. Animals were irradiated 12 h before bone marrow reconstitution.

Bone marrow reconstitution assays. For competitive bone marrow repopulation assays[42], we co-transferred 2 × 10^6 whole bone marrow cells from CD45.1 mice after three weeks of stress or from nonstressed controls together with equal cell numbers of CD45.2 competitor cells from nonstressed wild-type mice into lethally irradiated UBC-GFP CD45.2 mice. Engraftment was assessed by comparing blood leukocyte chimerism for CD45.1 cells between groups after 2, 3 and 4 months. For limiting dilution experiments[42], donor doses of 1.5 × 10^4, 6 × 10^4, 12.5 × 10^4 or 5 × 10^5 whole bone marrow cells from CD45.1 mice after three weeks of stress or from nonstressed controls were co-transferred with 5 × 10^5 CD45.2 competitor cells into lethally irradiated CD45.2 recipients. Engraftment was assessed after four months as at least >0.1% multilineage blood chimerism for B lymphocytes, T lymphocytes and myeloid lineage cells derived from donor bone marrow. Poisson's statistic was calculated using L-calc software (Stemcell Technologies) and ELDA software[43]. Bone marrow of two mice was pooled for each cell population.

Treatment with adrenergic receptor antagonists. To inhibit β_3-adrenergic signaling, a specific antagonist for the β_3-adrenergic receptor (SR 59230A, Sigma-Aldrich) was injected at 5 mg/kg body weight i.p. twice per day[44]. For inhibition of β_2-adrenergic signaling, ICI118,551 hydrochloride (Sigma-Aldrich) was injected daily at a dose of 1 mg/kg body weight i.p. (ref. 18) for three weeks. The control groups received saline injections.

Depletion of sympathetic nerve fibers. TH-Cre mice were cross-bred with iDTR mice. 10–12 week old female TH-iDTR mice were intraperitoneally injected with 0.1 µg/kg body weight diphtheria toxin (DT) on day 0 and day 3 after initiation of stress procedures[18]. Age-matched littermates (TH-Cre, iDTR or WT) that were also stressed and injected with DT served as controls.

5-Fluorouracil challenge. Nonstressed mice and mice that had been stressed for three weeks were injected intravenously with 150 mg/kg body weight 5-FU (Sigma)[45] on day 0. Mice were then followed over the course of 21 days, and the absolute number of blood leukocytes was measured after 7, 14 and 21 days. Stress exposure continued for the remaining 3 weeks after 5-FU exposure.

Tissue processing. Flushed bone marrow was passed through a 40-µm cell strainer and collected in PBS containing 0.5% BSA and 1% FBS (FACS buffer). Aortas were excised, minced and digested in collagenase I (450 U/ml), collagenase XI (125 U/ml), DNase I (60 U/ml) and hyaluronidase (60 U/ml) (all Sigma-Aldrich) at 37 °C at 750 r.p.m. for 1 h. For sorting niche cells, bones were harvested from nestin-GFP mice. Bone marrow endothelial cells (ECs) and mesenchymal stem cells (MSCs) were obtained by flushing out bone marrow, which was then digested in 10 mg/ml collagenase type IV (Worthington) and 20 U/ml DNase I (Sigma)[46]. For obtaining bone osteoblastic lineage cells, we crushed bones, washed off residual bone marrow cells three times and then digested and incubated the bone fragments[47,48].

Flow cytometry. For myeloid cells, cells were first stained with mouse hematopoietic lineage markers (1:600 dilution for all antibodies) including phycoerythrin (PE) anti-mouse antibodies directed against B220 (BD Bioscience, clone RA3-6B2), CD90 (BD Bioscience, clone 53-2.1), CD49b (BD Bioscience, clone DX5), NK1.1 (BD Bioscience, clone PK136) and Ter-119 (BD Bioscience, clone TER-119). This was followed by a second staining for CD45.2 (BD Bioscience, clone 104, 1:300), CD11b (BD Bioscience, clone M1/70, 1:600), CD115 (eBioscience, clone M1/70, 1:600), Ly6G (BD Bioscience, clone 1A8, 1:600), CD11c (eBioscience, clone HL3, 1:600), F4/80 (Biolegend, clone BM8, 1:600) and Ly6C (BD Bioscience, clone AL-21, 1:600). Neutrophils were identified as (CD90/B220/CD49b/NK1.1/Ter119)^{low}(CD45.2/CD11b)^{high}CD115^{low}Ly6G^{high}. Monocytes were identified as (CD90/B220/CD49b/NK1.1/Ter119)^{low}CD11b^{high}(F4/80/CD11c)^{low}Ly-6C$^{high/low}$ or (CD45.2/CD11b)^{high}Ly6G^{low}CD115^{high}Ly-6C$^{high/low}$. Macrophages were identified as (CD90/B220/CD49b/NK1.1/Ter119)^{low}CD11b^{high}Ly6C$^{low/int}$ Ly6G^{low}F4/80^{high}. For hematopoietic progenitor staining, we first incubated cells with biotin-conjugated anti-mouse antibodies (1:600 dilution for all antibodies) directed against B220 (eBioscience, clone RA3-6B2), CD11b (eBioscience, clone M1/70), CD11c (eBioscience, clone N418), NK1.1 (eBioscience, clone PK136), TER-119 (eBioscience, clone TER-119), Gr-1 (eBioscience, clone RB6-8C5), CD8a (eBioscience, clone 53-6.7), CD4 (eBioscience, clone GK1.5) and IL7Rα (eBioscience, clone A7R34) followed by pacific orange–conjugated streptavidin anti-biotin antibody. Then cells were stained with antibodies directed against c-Kit (BD Bioscience, clone 2B8, 1:600), Sca-1 (eBioscience, clone D7, 1:600), SLAM markers[10] CD48 (eBioscience, clone HM48-1, 1:300) and CD150 (Biolegend, clone TC15-12F12.2, 1:300), CD34 (BD Bioscience, clone RAM34, 1:100), CD16/32 (BD Bioscience, clone 2.4G2, 1:600) and CD115 (eBioscience, clone AFS98, 1:600). LSKs were identified as (B220

doi:10.1038/nm.3589

CD11b CD11c NK1.1 Ter-119 Ly6G CD8a CD4 IL7Rα)^{low}c-Kit^{high}Sca-1^{high}. HSCs were identified as (B220 CD11b CD11c NK1.1 Ter-119 Ly6G CD8a CD4 IL7Rα)^{low}c-Kit^{high}Sca-1^{high}CD48^{low}CD150^{high}. Granulocyte macrophage progenitors were defined as (B220 CD11b CD11c NK1.1 Ter-119 Ly6G CD8a CD4 IL7Rα)^{low}c-Kit^{high}Sca-1^{low}(CD34/CD16/32)^{high}CD115$^{int/low}$. Macrophage dendritic cell progenitors were defined as (B220 CD11b CD11c NK1.1 Ter-119 Ly6G CD8a CD4 IL7Rα)^{low}c-Kit$^{int/high}$Sca-1^{low}(CD34/CD16/32)^{high}CD115^{high}. Common lymphoid progenitors were identified as (B220 CD11b CD11c NK1.1 Ter-119 Ly6G CD8a CD4)^{low}c-Kit^{int}Sca-1^{int}IL7Rα^{high}. For staining endothelial cells, we used ICAM-1 (Biolegend, clone Yn1/1.7.4, 1:300), ICAM-2 (Biolegend, clone 3C4, 1:300), VCAM-1 (Biolegend, clone 429, 1:300), E-selectin (CD62E) (BD Bioscience, clone 10E9.6, 1:100), P-selectin (CD62P) (BD Bioscience, clone RB40.34, 1:100), CD31 (Biolegend, clone 390, 1:600), CD107a (LAMP-1) (Biolegend, clone 1D4B, 1:600) and CD45.2 (Biolegend, clone 104, 1:300). Streptavidin–pacific orange was used to label biotinylated antibodies. Endothelial cells were identified as CD45.2^{low}, CD31^{high} and CD107a$^{intermed/high}$. For analysis of human monocyte subsets, cells were stained for HLA-DR (Biolegend, clone L243, 1:600), CD16 (Biolegend, clone 3G8, 1:600) and CD14 (Biolegend, clone HCD14, 1:600) after red blood cell lysis (RBC Lysis buffer, Biolegend). Monocytes were identified using forward and side scatter as well as HLA-DR. Within this population, frequencies of monocyte subsets CD14^{high}, CD16^{high} and CD14^{high}/CD16^{high} were quantified.

BrdU experiments. For BrdU pulse experiments, we used APC/FITC BrdU flow kits (BD Bioscience). One mg BrdU was injected i.p. 24 h before organ harvest. BrdU staining was performed according to the manufacturer's protocol. For BrdU application over 7 days, osmotic micropumps (Alzet) filled with 18mg BrdU were implanted. For the BrdU label-retaining pulse chase assay, BrdU was added to drinking water (1 mg/ml) for 17 days[11].

Cell cycle analysis. After surface staining, intracellular staining was performed according to eBioscience's protocol: cells were fixed and permeabilized using the Foxp3/Transcription Factor Staining Buffer Set (eBioscience) and then stained for the nuclear antigen Ki-67 (eBioscience, clone SolA15). Cell cycle status was determined using 4,6-diamidino-2-phenylindole (DAPI, FxCycle Violet Stain, Life Technologies).

Cell sorting. To isolate HSPCs, we used MACS depletion columns (Miltenyi) after incubation with a cocktail of biotin-labeled antibodies (as described in the flow cytometry section) followed by incubation with streptavidin-coated microbeads (Miltenyi). Next, cells were stained with c-Kit and Sca-1, and LSKs were FACS-sorted using a FACSAria II cell sorter (BD Biosystems). To purify niche cells from hematopoietic cells, we used MACS depletion columns after incubation with a cocktail of biotin-labeled antibodies as above followed by incubation with streptavidin-coated microbeads. Cells were then stained with CD45.2, Sca-1, CD31 and CD51 (Biolegend, clone RMV-7, 1:100). Endothelial cells were identified as Lin^{low}CD45^{low}Sca-1^{high}CD31^{high}. Bone marrow MSCs were identified as Lin^{low}CD45^{low}CD31^{low}Sca-1$^{high/intermediate}$ and GFP^{+}. Osteoblasts were Lin^{low}CD45^{low}Sca-1^{low}CD31^{low}CD51^{high}. For adoptive transfer of GFP^{+} neutrophils and Ly6C^{high} monocytes, bone marrow cells were collected from UBC-GFP mice for purification of neutrophils and monocytes using MACS depletion columns after incubation with a cocktail of PE–labeled antibodies including B220, CD90, CD49b, NK1.1 and Ter-119 followed by an incubation with PE-coated microbeads. Aortic endothelial cells were identified as CD45.2^{low}CD31^{high}CD107a$^{int/high}$ and FACS-sorted using a FACSAria II cell sorter.

Adoptive transfer. We injected 2 × 10^{6} neutrophils together with 2 × 10^{6} Ly6C^{high} monocytes intravenously into nonstressed and stressed *Apoe*$^{-/-}$ mice (the mice were stressed for 6 weeks, and the cells were injected 2 days before the end of the 6 weeks). Aortas were harvested 48 h later. The number of CD11b^{high}GFP^{+} cells within the aorta was quantified using flow cytometry.

Histology. Aortic roots were harvested and embedded to produce 6-µm sections that were stained using an anti-CD11b (BD Biosciences, clone M1/70, 1:15 dilution) or anti-Ly6G (Biolegend, clone 1A8, 1:25 dilution) antibody followed with a biotinylated secondary antibody. For color development, we used the VECTA STAIN ABC kit (Vector Laboratories, Inc.) and AEC substrate (DakoCytomation). Necrotic core and fibrous cap thickness were assessed using Masson trichrome (Sigma) staining. Necrotic core was evaluated by measuring the total acellular area within each plaque. For fibrous cap thickness, three to five measurements representing the thinnest part of the fibrous cap were averaged for each plaque as previously described[49]. For tyrosine hydroxylase staining, femurs were harvested and fixed in 4% paraformaldehyde for 3 h and then decalcified in 0.375 M EDTA in PBS for 10 days before paraffin embedding. Sections were cut and stained with anti–tyrosine hydroxylase antibody (Millipore, AB152, dilution 1:100) after deparaffinization and rehydration. Sections were scanned with NanoZoomer 2.0-RS (Hamamatsu) at 40× magnification and analyzed using IPLab (Scanalytics).

Intravital microscopy. For intravital microscopy of hematopoietic progenitors in the bone marrow of the calvarium, LSKs were isolated from either wild-type C57BL/6 or C57BL/6-Tg(UBC-GFP)30Scha/J mice and labeled with the lipophilic membrane dye DiD (1,1′-dioctadecyl-3,3,3′,3′-tetramethylindodicarbocyanine perchlorate, Invitrogen). 25,000 labeled LSKs were transferred i.v. into nonirradiated C57BL/6 recipient mice. For blood pool contrast, TRITC–dextran (Sigma) was injected immediately before imaging. OsteoSense 750 (PerkinElmer) was injected i.v. 24 h before *in vivo* imaging to outline bone structures in the calvarium[50]. *In vivo* imaging was performed on days 1 and 7 after the adoptive cell transfer using an IV100 confocal microscope (Olympus)[15]. Three channels were recorded (DiD excitation/emission 644/665 nm, OsteoSense 750 excitation/emission 750/780 nm, TRITC–Dextran excitation/emission 557/576 nm) to generate *z* stacks of each location at 2-µm steps. Image postprocessing was performed using Image J software. Mean DiD fluorescence intensity was measured for each labeled cell and then normalized to the background by calculating the target to background ratio.

Colony-forming unit assay. Colony-forming unit (CFU) assays were performed using a semisolid cell culture medium (Methocult M3434, Stem Cell Technology) following the manufacturer's protocol. Bones were flushed with Iscove's Modified Dulbecco's Medium (Lonza) supplemented with 2% FCS. 2 × 10^{4} bone marrow cells were plated on a 35-mm plate in duplicates and incubated for 7 days. Colonies were counted using a low magnification inverted microscope.

Blood pressure and heart rate measurement. Blood pressure and heart rate were measured using a noninvasive tail-cuff system (Kent Scientific Corporation) according to the manufacturer's instructions. For each value, the mean of three consecutive measurements was used.

Quantitative real-time PCR. Messenger RNA (mRNA) was extracted from aortic arches or bone marrow using the RNeasy Mini Kit (Qiagen) or from FACS-sorted cells using the Arcturus PicoPure RNA Isolation Kit (Applied Biosystems) according to the manufacturers' protocol. One microgram of mRNA was transcribed to complementary DNA (cDNA) with the high capacity RNA to cDNA kit (Applied Biosystems). We used Taqman primers (Applied Biosystems). Results were expressed by Ct values normalized to the housekeeping gene *Gapdh*.

Fluorescence molecular tomography–computed tomography. After six weeks of stress, FMT-CT imaging was performed and compared to nonstressed, age-matched *Apoe*$^{-/-}$ controls. Pan-cathepsin protease sensor (Prosense-680, PerkinElmer, 5 nmol) was injected intravenously 24 h before the imaging as previously described[51].

ELISA. Blood corticosterone levels were measured by ELISA (Abcam). Serum was collected between 10 a.m. and 12 p.m. For measurements of noradrenaline in the bone marrow, a 2–CAT (A–N) Research ELISA (Labor Diagnostika Nord) was used. One femur was snap-frozen and immediately homogenized in a catecholamine stabilizing solution containing sodium metabisulfite (4 mM), EDTA (1 mM) and hydrochloric acid (0.01 N). Prior to the ELISA, the

pH of the sample was adjusted to 7.5 using sodium hydroxide (1 N). ELISAs for CXCL12 (R&D), IFN-α (PBL Biomedical Laboratories) and IFN-γ (R&D) in the bone marrow were performed using one femur and one tibia per mouse[14]. ELISAs were performed according to the manufacturers' instructions.

Statistical analyses. Statistical analyses were performed using GraphPad Prism software (GraphPad Software, Inc.). Results are depicted as mean ± standard error of mean if not stated otherwise. For a two-group comparison, a Student's *t*-test was applied if the pretest for normality (D'Agostino-Pearson normality test) was not rejected at the 0.05 significance level; otherwise, a Mann-Whitney *U* test for nonparametric data was used. For a comparison of more than two groups, an ANOVA test, followed by a Bonferroni test for multiple comparison, was applied. For analysis of clinical data, a Wilcoxon test for matched pairs was used. *P* values of <0.05 indicate statistical significance. No statistical method was used to predetermine sample size.

41. Encinas, J.M *et al.* Division-coupled astrocytic differentiation and age-related depletion of neural stem cells in the adult hippocampus. *Cell Stem Cell* **8**, 566–579 (2007).
42. Purton, L.E. & Scadden, D.T. Limiting factors in murine hematopoietic stem cell assays. *Cell Stem Cell* **1**, 263–270 (2007).
43. Hu, Y. & Smyth, G.K. ELDA: extreme limiting dilution analysis for comparing depleted and enriched populations in stem cell and other assays. *J. Immunol. Methods* **347**, 70–78 (2009).
44. Dutta, P. *et al.* Myocardial infarction accelerates atherosclerosis. *Nature* **487**, 325–329 (2012).
45. Kobayashi, M. & Srour, E.F. Regulation of murine hematopoietic stem cell quiescence by Dmtf1. *Blood* **118**, 6562–6571 (2011).
46. Shi, C. *et al.* Bone marrow mesenchymal stem and progenitor cells induce monocyte emigration in response to circulating Toll-like receptor ligands. *Immunity* **34**, 590–601 (2011).
47. Westerterp, M. *et al.* Regulation of hematopoietic stem and progenitor cell mobilization by cholesterol efflux pathways. *Cell Stem Cell* **11**, 195–206 (2012).
48. Schepers, K. *et al.* Myeloproliferative neoplasia remodels the endosteal bone marrow niche into a self-reinforcing leukemic niche. *Cell Stem Cell* **13**, 285–299 (2013).
49. Seimon, T.A. *et al.* Macrophage deficiency of p38α MAPK promotes apoptosis and plaque necrosis in advanced atherosclerotic lesions in mice. *J. Clin. Invest.* **119**, 886–898 (2009).
50. Zaheer, A. *et al. In vivo* near-infrared fluorescence imaging of osteoblastic activity. *Nat. Biotechnol.* **19**, 1148–1154 (2001).
51. Nahrendorf, M. *et al.* Hybrid PET-optical imaging using targeted probes. *Proc. Natl. Acad. Sci. USA* **107**, 7910–7915 (2010).

doi:10.1038/nm.3589